One-dimensional arrays of nanoshell dimers for single molecule spectroscopy via surface-enhanced raman scattering

Ke Zhao
Department of Physics and Astronomy, The University of Tennessee, Knoxville, Tennessee 37996

Hongxing Xu
Institute of Physics, Chinese Academy of Sciences, Beijing, 100080 People's Republic of China and Division of Solid State Physics, Lund University, Lund, SE-22100 Sweden

Baohua Gu
Environmental Sciences Division, Oak Ridge National Laboratory, Oak Ridge, Tennessee 37831

Zhenyu Zhang
Materials Science and Technology Division, Oak Ridge National Laboratory, Oak Ridge, Tennessee 37831; Department of Physics and Astronomy, The University of Tennessee, Knoxville, Tennessee 37996 and Division of Engineering and Applied Sciences, Harvard University, Cambridge, Massachusetts 02138

(Received 30 March 2006; accepted 22 June 2006; published online 25 August 2006)

The optical properties of one-dimensional arrays of metal nanoshell dimers are studied systematically using the T-matrix method based on Mie theory, within the context of surface enhanced Raman scattering (SERS). It is shown that the local electromagnetic enhancement can be as high as $\sim 4.5 \times 10^{13}$ for nanoshell dimer arrays with optimal geometry, and sensitive tunability in the resonant frequency can be gained by varying the geometrical parameters, making such structures appealing templates for SERS measurements with single molecule sensitivity. The extraordinarily high enhancement is attributed to a collective photonic effect constructively superposed onto the intrinsic enhancement associated with an isolated nanoshell dimer. © *2006 American Institute of Physics*. [DOI: 10.1063/1.2229204]

Extensive studies have been focused on surface enhanced Raman scattering (SERS), referring to the phenomenon that molecules adsorbed on a roughened metal substrate exhibit much higher Raman scattering cross sections than in the gaseous phase (typically enhanced by the order of 10^6).[1] Recent experiments have observed even greater Raman enhancement when certain biological or organic dye molecules were trapped in the gap region (so-called the "hot spot") between two very closely placed solid metal nanoclusters.[2,3] Here the enhancement factors could be greater than 10^{10}, thereby rendering SERS as potentially an ultra-sensitive analytical tool for single molecule spectroscopy (SMS).[2–5]

At the other front, the field of nanofabrication has witnessed tremendous progresses over the last decade. One compelling example is the successful fabrication of nanoshells, consisting of dielectric cores coated with metal shells that can be only a few nanometers in thickness.[6,7] When used as templates, such metal nanoshells can yield even higher Raman enhancement than solid metal nanoclusters, particularly in the dimer geometry.[8] Furthermore, the metal nanoshells have an added tunability for SRES applications, in which the resonant wavelength for maximal SERS enhancement can be tuned by changing the shell thickness.[9–11]

To date, the enormous Raman enhancement has been obtained experimentally only from a few Raman active metal-nanocluster (solid or shell) dimers randomly distributed among large ensembles of nanoclusters; therefore, only random spatial correlations existed among the dimers.[2,3,8] Nevertheless, it is conceivable that, as the fields of SERS and nanofabrication both advance, highly ordered metal nanocluster dimer arrays with delicate tunability in geometry will be fabricated. Such ordered dimer arrays will not only offer new opportunities to expand fundamental studies of SERS, but also broaden the range of SERS applications, particularly in chemical and biological sciences.[2,12]

It has been widely accepted that two primary effects contribute to SERS: electromagnetic (EM) and chemical effects.[1,13] The EM effect refers to the enhancement, relative to the incident field, in the local electromagnetic field near the roughened metal substrate due to the optical response of the substrate. Such an enhancement is particularly large in the gap region of two very closely placed nanoclusters.[8,14–16] To a good approximation, the EM enhancement is given by $|\vec{E}_{\mathrm{loc}}/\vec{E}_0|^4$, where $\vec{E}_{\mathrm{loc}}$ is the local electric field felt by an adsorbed molecule and is the superposition of the scattered field $\vec{E}_{\mathrm{sc}}$ and incident field $\vec{E}_0$: $\vec{E}_{\mathrm{loc}}=\vec{E}_0+\vec{E}_{\mathrm{sc}}$. The chemical effect is typically attributed to nonadiabatic charge transfer processes.[17–19] Of the two, the EM effect dominates and can be over 10^{10} in the so-called "nanoneck" region of a nanocluster dimer, while the chemical effect usually accounts for an additional enhancement of the order $\sim 10^2$ when charge transfer processes take place.[17–19]

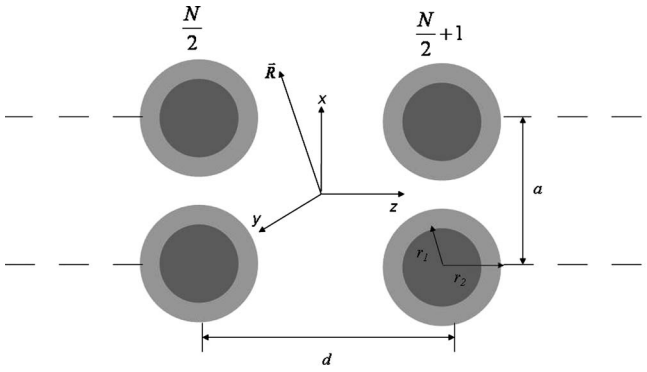

FIG. 1. Geometrical illustration of an ordered one-dimensional array of metal nanoshell dimers.

In this letter, we systematically study the optical properties of ordered one-dimensional (1D) arrays of silver nanoshell dimers using the T-matrix method based on Mie theory.[20,21] Our focus is on the contribution of the EM field enhancement to SERS. We show that the EM enhancement can be as high as $\sim 4.5\times 10^{13}$ for nanoshell dimer arrays with optimal geometry, making such structures highly desirable templates for single molecule spectroscopy via SERS. The extraordinarily high EM enhancement is attributed to a long-range collective photonic effect associated with the array structure, constructively superposed onto the intrinsic enhancement associated with an isolated nanoshell dimer. We compare the results with those from ordered 1D arrays of solid metal nanocluster dimers, and illustrate the sensitive tunability in the resonant frequency gained by the use of the nanoshell templates.

The basic geometry of the model system is illustrated in Fig. 1. Silver nanoshell dimers are aligned to form a 1D array, with the dimer axes perpendicular to the array direction. Taking advantage of the superposition principle, we treat the incident light as plane waves of frequency $\omega = (2\pi)/\lambda$, where λ is the wavelength. The polarization of the incident wave is chosen to be parallel to the dimer axes, while the wave vector is perpendicular to the array direction. For mathematical simplicity without losing generality, we also treat the array to be infinitely long, making the system translationally invariant. This approximation is valid because our focus is on the central region of a long enough dimer array. Within the T-matrix method, the scattered field $\vec{E}_{\rm sc}(\omega,\vec{R})$ in response to the incident wave from the array can be expressed as the superposition of scattered fields from all the individual spheres,

$$\vec{E}_{\rm sc}(\omega,\vec{R}) = \sum_{\eta=1,2}\sum_{n=1}^{\infty}\sum_{m=-n}^{n}\sum_{l=1}^{N\to\infty}\left[\alpha_{mn}^{\eta}(l)\cdot\vec{N}_{mn}^{(3)}(\omega,\vec{r}_l^{\eta}) + \beta_{mn}^{\eta}(l)\cdot\vec{M}_{mn}^{(3)}(\omega,\vec{r}_l^{\eta})\right], \tag{1}$$

where η represents the different spheres in each individual dimer, l is the index of different dimers, N is the total number of dimers, $\vec{N}_{mn}^{(3)}(\omega,\vec{r})$ and $\vec{M}_{mn}^{(3)}(\omega,\vec{r})$ are the normal modes, which contain the first kind of Hankel functions in their radial parts and spherical harmonics of indices m and n in their angular parts,[21] $\alpha_{mn}^{\eta}(l)$ and $\beta_{mn}^{\eta}(l)$ are the expansion coefficients. In Eq. (1), the position vector $\vec{R}$ is defined relative to the center of the whole array (see Fig. 1), and $\vec{r}_l^{\eta}=\vec{R}+(N/2-l+0.5)d\cdot\hat{z}+(\eta-1.5)a\cdot\hat{x}$ is defined relative to the center of the ηth sphere in the lth dimer, d is the inter-dimer distance, and a is the distance between the two sphere centers within a dimer. Invoking the periodic boundary condition, we have $\gamma_{mn}^{\eta}(l)=\gamma_{mn}^{\eta}(l+N)$ and $\gamma_{mn}^{\eta}(l)=\Sigma_h\tilde{\gamma}_{mn}^{\eta}(h)\cdot\exp(ihld)$, where $\gamma=\alpha,\beta$, $h=(2\pi/Nd)s$ is the wave vector defined within the first Brillouin zone, and s is given by $-N/2\le s<N/2$ (here we have further assumed N is even for convenience).

The expansion coefficients $\tilde{\alpha}_{mn}^{\eta}(h)$ and $\tilde{\beta}_{mn}^{\eta}(h)$ are further determined by:

$$\tilde{\alpha}_{mn}^{\eta}(h) = \upsilon_n\left\{p_{mn}^0\delta_{0,h} + \sum_{\nu=1}^{\infty}\sum_{\mu=-\nu}^{\nu}\left[\tilde{\alpha}_{\mu\nu}^{\eta}(h)\cdot\left(\sum_{\bar{l}}\exp(ih\bar{l}d)\cdot A_{mn}^{\mu\nu}(\bar{l},\eta\eta)\right) + \tilde{\beta}_{\mu\nu}^{\eta}(h)\cdot\left(\sum_{\bar{l}}\exp(ih\bar{l}d)\cdot B_{mn}^{\mu\nu}(\bar{l},\eta\eta)\right)\right.\right.$$
$$\left.\left. + \tilde{\alpha}_{\mu\nu}^{\xi}(h)\cdot\left(\sum_{\bar{l}}\exp(ih\bar{l}d)\cdot A_{mn}^{\mu\nu}(\bar{l},\eta\xi)\right) + \tilde{\beta}_{\mu\nu}^{\xi}(h)\cdot\left(\sum_{\bar{l}}\exp(ih\bar{l}d)\cdot B_{mn}^{\mu\nu}(\bar{l},\eta\xi)\right)\right]\right\} \tag{2a}$$

$$\tilde{\beta}_{mn}^{\eta}(h) = u_n\left\{q_{mn}^0\delta_{0,h} + \sum_{\nu=1}^{\infty}\sum_{\mu=-\nu}^{\nu}\left[\tilde{\alpha}_{\mu\nu}^{\eta}(h)\cdot\left(\sum_{\bar{l}}\exp(ih\bar{l}d)\cdot B_{mn}^{\mu\nu}(\bar{l},\eta\eta)\right) + \tilde{\beta}_{\mu\nu}^{\eta}(h)\cdot\left(\sum_{\bar{l}}\exp(ih\bar{l}d)\cdot A_{mn}^{\mu\nu}(\bar{l},\eta\eta)\right)\right.\right.$$
$$\left.\left. + \tilde{\alpha}_{\mu\nu}^{\xi}(h)\cdot\left(\sum_{\bar{l}}\exp(ih\bar{l}d)\cdot B_{mn}^{\mu\nu}(\bar{l},\eta\xi)\right) + \tilde{\beta}_{\mu\nu}^{\xi}(h)\cdot\left(\sum_{\bar{l}}\exp(ih\bar{l}d)\cdot A_{mn}^{\mu\nu}(\bar{l},\eta\xi)\right)\right]\right\} \tag{2b}$$

where u_n and v_n are the Mie coefficients,[22] p^0_{mn} and q^0_{mn} are the expansion coefficients of the normal modes $\vec{N}^{(1)}_{mn}(\omega,\vec{r})$ and $\vec{M}^{(1)}_{mn}(\omega,\vec{r})$ for the incident wave, where $\vec{N}^{(1)}_{mn}(\omega,\vec{r})$ and $\vec{M}^{(1)}_{mn}(\omega,\vec{r})$ contain the first kind of Bessel functions in their radial parts.[21] $A^{\mu\nu}_{mn}(\bar{l},\eta\xi)$ and $B^{\mu\nu}_{mn}(\bar{l},\eta\xi)$ are the coefficients of the coordinate transform from the origin of the ξth sphere in the lth dimer to the ηth sphere in the lth dimer,[23] with $\eta \neq \xi=1,2$ and $\bar{l}=l'-l$ summing over all the relative positions of the spheres. Note that by definition, $A^{\mu\nu}_{mn}(0,\eta\eta)=0$ and $B^{\mu\nu}_{mn}(0,\eta\eta)=0$. In our calculations, n and ν are truncated to the maximum multipole value of L, and $\bar{l}$ is truncated to a maximum number of neighboring dimers. Detailed tests show that the choices of $L=20$ and $\bar{l}=200$ will guarantee adequate numerical convergence in most cases (exceptions are discussed below).

Using the above formalism, we now investigate the optical properties of the arrays of nanoshell dimers by varying the inter-dimer distance d and the shell geometry (r_1,r_2), where r_1 and r_2 are the inner and outer radius of the shells, respectively. To draw those comparison with the results for isolated solid nanocluster dimer or dimer arrays,[14–16,24] we first focus on the cases where the nanoneck distance between the two spheres of an individual nanoshell dimer is fixed at 1 nm. The essential physics to be elucidated, namely, the collective photonic effect, is insensitive to the precise choice of this separation. Later, we will also consider the more practical case where the separation is increased to 3 nm. The dielectric core is chosen to be silica, with a dielectric constant of $\varepsilon=2.56$. The frequency dependence of the dielectric constant of the silver shell is approximated by the experimental data for bulk silver unless otherwise specified.[25] This approximation is supported by recent experimental data,[26] though the imaginary part of the dielectric function of a metal shell, can be different from its bulk value due to factors such as electron scattering at the interfaces.[27]

Figure 2(a) shows the EM enhancement, M versus the wavelength λ at the location half way between the shell centers of a dimer in a nanoshell array with the fixed shell geometry of ($r_1=35$ nm, $r_2=38$ nm) but different inter-dimer distances d. For every d, there are multiple enhancement peaks. The maximum enhancement of $M=4.5\times10^{13}$ is obtained for the optimal inter-dimer distance of $d=950$ nm, above which the enhancement factor decreases from the maximum value. Note that, as d changes from 216 to 950 nm, the maximum enhancement peak also exhibits a weak red shift resulting from a delicate long-range collective photonic effect, as detailed below.

For comparison, the intrinsic EM enhancement of an isolated dimer with the same shell geometry as that of the dimers in the array, is shown in Fig. 2(a). The maximum enhancement of $M_i=5\times10^{12}$ for the isolated dimer is about one order of magnitude smaller than the enhancement for the optimal dimer array. In general, for each nanoshell dimer geometry of (a,r_1,r_2), one can always optimize the inter-dimer distance in the array structure to gain $1\sim2$ orders of magnitude of additional enhancement on top of that from the isolated dimer. Here we introduce M_a to measure the additional enhancement, defined as $M=M_i\cdot M_a$, as plotted in Fig.

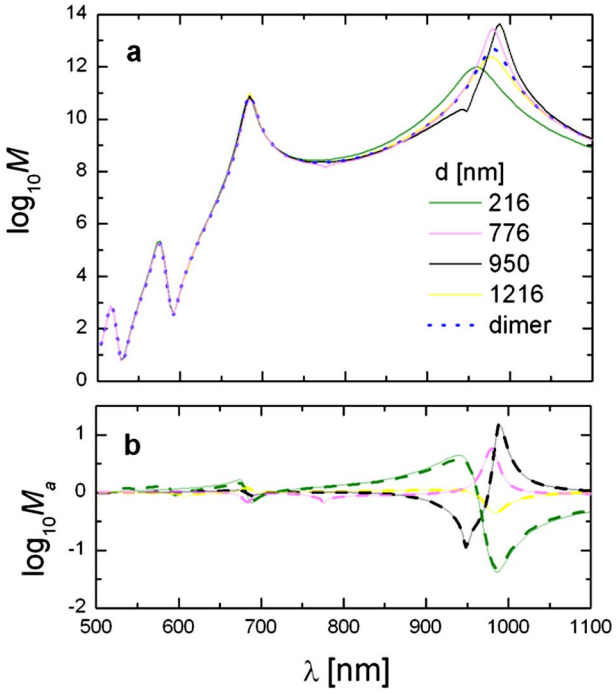

FIG. 2. (a) EM enhancements vs the wavelength of the incident light at the location half way between the two centers of a metal nanoshell dimer in dimer arrays of different inter-dimer distances. The dotted line is for an isolated dimer of identical geometry. (b) Solid lines: the additional enhancements due to long-range photonic effects, given by the subtractions of the dotted line in (a) from the solid lines, also in (a). The dashed lines are the results from the dipole approximation expressed by Eq. (3).

2(b) for different array geometries. When the additional enhancement is sufficiently large and also near the resonant wavelength for maximum enhancement from the isolated dimer, a net enhancement over the isolated dimer value can be achieved from the array, as in the case of $d=776$ and 950 nm. Such additional enhancements are the results of a long-range collective photonic effect, which can be understood within the picture of coupled dipoles.[28] When the incident wavelength λ and the separation d between two neighboring dimers are much larger than the dimer size, the dimers can generate nearly homogeneous dipolar electromagnetic field on each other. With the incident polarization parallel to the axes of the dimers, the effective external field on any dimer in the array is:

$$\vec{E}_{0,\mathrm{eff}}(\omega)=\frac{\vec{E}_0(\omega)}{1-2\alpha(\omega)\cdot\sum_{|\bar{l}|}R(\omega,|\bar{l}|)\exp(i\omega/c|\bar{l}|d)}, \tag{3}$$

where $\alpha(\omega)$ is the polarizability of an isolated dimer obtained by calculating the electric field sufficiently away from this dimer using the T-matrix method and then fitting the results in the dipole approximation. In Eq. (3), $R(\omega,|\bar{l}|)=\{\omega^2/(c^2|\bar{l}|d)-1/(|\bar{l}|d)^3+i\omega/[c(|\bar{l}|d)^2]\}$, c is the speed of light in vacuum. Thus, the additional enhancement can be calculated by $M_a=|\vec{E}_{0,\mathrm{eff}}(\omega)|^4/|\vec{E}_0(\omega)|^4$. As shown by the dashed lines in Fig. 2(b), the additional enhancements obtained from the coupled dipole approximation agree very well with the results from the exact T-matrix calculations; the

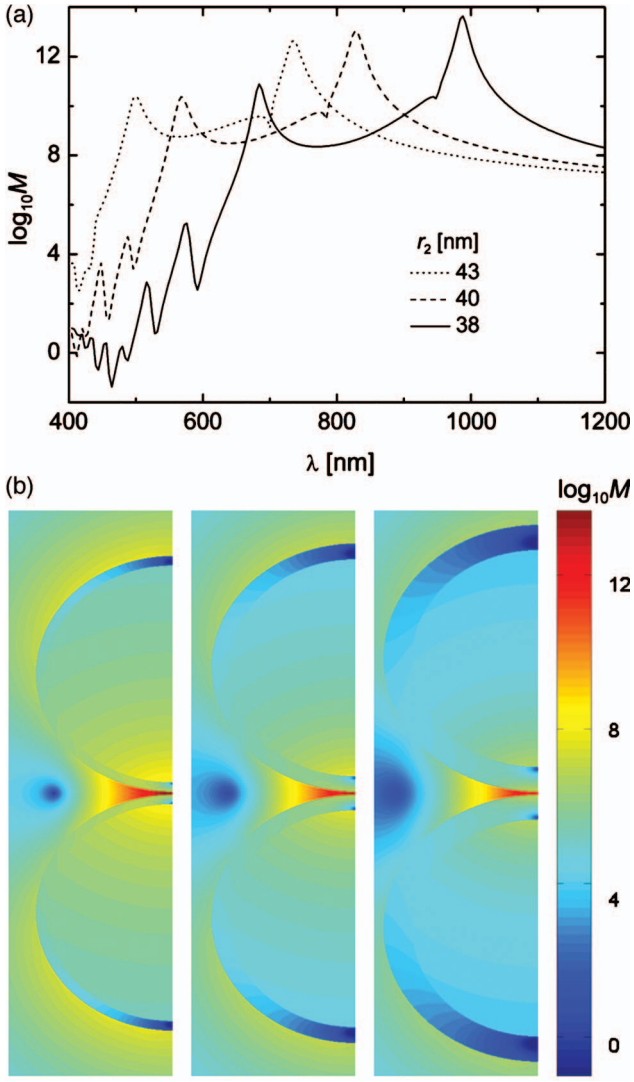

FIG. 3. (Color) (a) Same as in Figure 2(a), but with different outer radii of the nanoshells. (b) Color illustration of the EM enhancement in the symmetry plane defined by the dimer axes and the array direction, for the same geometries as in (a) (namely, r_2=38 nm (left), 40 nm (middle), 43 nm (right)), and at the different resonance wavelengths of 988, 828 and 736 nm, respectively.

differences are $<0.5\%$ for $d>200$ nm. Due to its far field nature, the additional enhancement is substantially smaller in magnitude than the intrinsic enhancement from the isolated dimer itself. Nevertheless, since the resonant wavelength for the additional enhancement is not necessarily the same as that for the intrinsic enhancement of an isolated dimer, a shift in the resonant wavelength of the whole array from that of the isolated dimer may occur, as shown in Fig. 2(a), for the cases d=216 and 950 nm.

We note that, if the wavelength of the incident light is nearly equal to the inter-dimer distance, $\exp[i(\omega/c)|\bar{l}|d] \sim 1$ in Eq. (3), and the summation of $R(\omega,|\bar{l}|)$ over $|\bar{l}|$ will not cancel out at large $|\bar{l}|$, explaining the singularities in Figs. 2, 3(a), and 4. Indeed, if we sum over $|\bar{l}|$ up to 20 000 at those specific frequencies, we can still observe $\sim 1\%$ change in the enhancement; in contrast, away from these specific frequencies, the enhancements are well converged when summing over $|\bar{l}|$ up to 200.

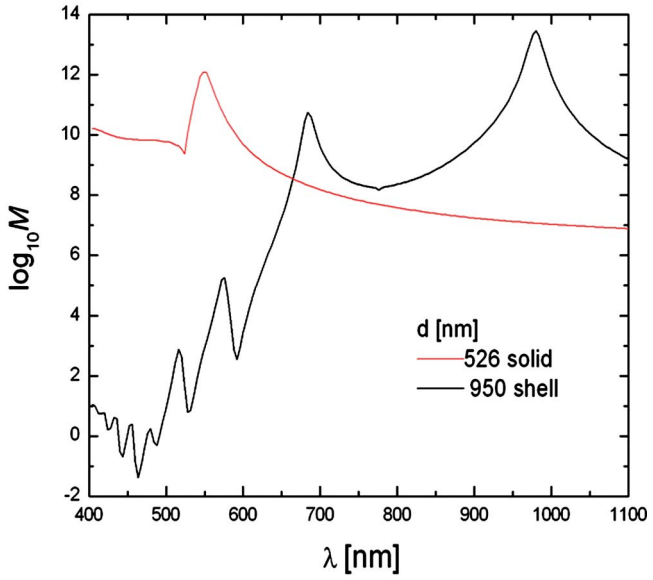

FIG. 4. Comparison of the EM enhancement from a one-dimensional array of solid spherical dimers and nanoshell dimers, respectively, as specified in the text. The different array structures require different inter-dimer distances for maximal enhancement, as indicated.

It has been shown previously that the plasmon resonance frequency of an isolated metal nanoshell strongly depends on its geometry.[10] Since the plasmon modes are largely responsible for the EM enhancement in SERS, we expect additional tunability in the SERS resonance frequency due to the shell geometry of a nanoshell array. Figure 3 shows the EM enhancement in arrays of nanoshell dimers with the same inner radius of r_1=35 nm but with different outer radii of r_2=38, 40, and 43 nm. The corresponding optimal inter-dimer distances are determined to be d=950, 785, and 701 nm, respectively. The resonant wavelength has a blue shift of about 260 nm when the outer radius of the shell increases from r_2=38 nm to r_2=43 nm. The typical EM enhancement of around 10^{13} achievable within a broad region of the resonance frequency is a very appealing feature of the shell arrays as templates for SERS measurements with single molecule sensitivity. In particular, as shown in Fig. 3(b), the effective "hot volume", defined by the collection of the hot spots in the nanogap region with an enhancement factor of 10^{10} or higher, is about 1713 nm^3 for r_2=38 nm, thereby providing a great potential for ultra-sensitive molecular spectroscopy by SERS.

Next, we compare the results from nanoshell dimer arrays with those from other related array structures. First, previous studies had shown that one-dimensional arrays of solid metal nanoclusters (or monomers) would produce a much lower EM enhancement than the nanoshell dimer arrays.[24,29] A closer analogy is that of the ordered 1D arrays of solid metal dimers. Figure 4 contrasts our simulation results for an array of solid silver dimers with identical dimer geometry of (a=77 nm, r_2=38 nm) as for the dimer shells, except for the value of r_1 (0 versus 35 nm), and different optimal inter-dimer distances for maximal enhancement. The nanoshell dimer array not only yields around 2 orders of magnitude higher enhancement than the solid dimer array, but also in-

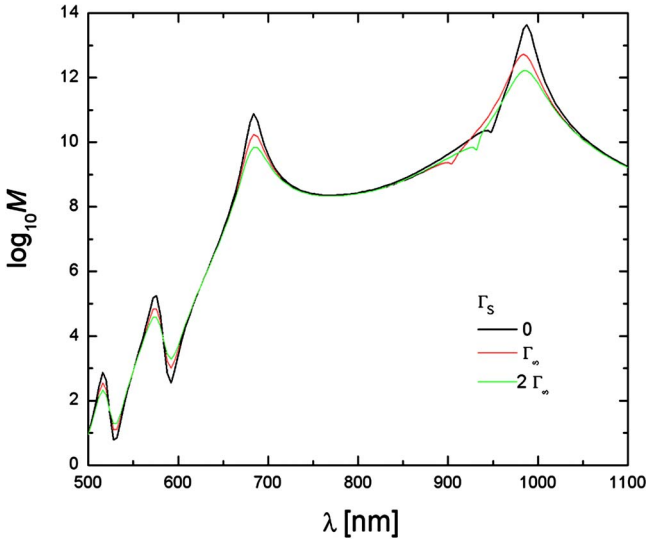

FIG. 5. EM enhancement vs wavelength for different broadening in the nanoshell dimer arrays, with shell geometry given by (r_1=35 nm, r_2=38 nm). For Γ_s=0, Γ_∞, $2\Gamma_\infty$, the optimal interdimer distance is d=950, 906 and 932 nm, respectively.

duces a dramatic shift in the resonance frequency.

As mentioned above, since the dielectric function of a nanoshell can differ quantitatively from its bulk value because electron scattering at the interfaces may introduce additional broadening, we study here how the spectrum is affected by such scattering. Empirically, using the Drude Model,[27] the dielectric function of the nanoshell can be described based on the bulk dielectric function, $\varepsilon_{Ag}(l,\omega)=\varepsilon_{Ag}(\omega)+\omega_p^2/(\omega^2+i\omega\Gamma_\infty)-\omega_p^2/[\omega^2+i\omega(\Gamma_\infty+\Gamma_s)]$, where $\varepsilon_{Ag}(\omega)=\varepsilon_{Ag}(\omega)_{\text{interband}}+(1-\omega_p^2/(\omega^2+i\omega\Gamma_\infty))$ is the dielectric function of bulk silver. Here $\hbar\omega_p$=9.2 eV is the bulk plasma energy in the Drude model,[30] $\Gamma_\infty=v_F/l_\infty$ is the collision frequency of conduction electrons in bulk silver, with $v_F=1.39\times10^6$ m/s the Fermi velocity and l_∞=52 nm the bulk mean free path.[30] Γ_s is the added electron collision frequency due to interface scattering. With no rigorous way to determine Γ_s at the present, we study quantitatively the effects of additional broadening on top of the standard bulk value by increasing the total electron collision frequency by 100% and 200% respectively. The results are shown in Fig. 5, for the nanoshell dimer array with radii (r_1=35 nm, r_2=38 nm) and optimal interdimer distances. When compared with the results for Γ_s=0, the maximum enhancement is lowered by 1 and 1.5 orders of magnitude for doubled and tripled broadening, respectively. Nevertheless, the maximum enhancement for either case is still well above 10^{11}. We therefore stress that, whereas such additional broadening would indeed lower the overall enhancement factor as expected, the two most salient features associated with the nanoshell dimer array geometry, namely, the distinct shift of resonant frequency into near infrared region and the collective photonic effect, remain valid.

Finally, as a comparison, we consider the case where the geometry of the nanoshells is unchanged (r_1=35 nm, r_2=38 nm), but the nanoneck distance is increase from 1–3 nm. Detailed calculations show that, at this larger gap separation, the maximum enhancement is decrease to $M=3.7\times10^{11}$, but the effective "hot volume" remains essentially the same (namely, changed from 1713–1730 nm^3). Such a large hot volume at the 3 nm gap separation makes the structures even more appealing for potential applications in ultra-sensitive molecular spectroscopy by SERS.

In conclusion, we have studied systematically the optical properties of ordered 1D arrays of silver nanoshell dimers using the T-matrix method based on Mie theory. We have shown that the EM contribution to SERS can be as high as $\sim4.5\times10^{13}$ for nanoshell dimer arrays with optimal geometry when additional broadening due to electron-interface scattering is not significant. The extraordinarily high enhancement is attributed to a long-range collective photonic effect associated with the array structure, constructively superposed onto the intrinsic enhancement associated with an isolated nanoshell dimer. The high EM enhancement, the large hot volume, and the sensitive tunability in the resonance frequency make such nanoshell array structures highly desirable templates for single molecule spectroscopy. Experimental work is currently in progress to test our theoretical predictions. With the rapid technological advances in nanofabrication,[31–34] we anticipate that such ideal next-generation SERS substrates consisting of highly ordered metal nanocluster (solid or shell) dimer arrays will soon be realized for a broad range of applications across different fields of studies.

We thank Mr. Zhipeng Li and Dr. Bo Persson for helpful discussions. We also thank Dr. Peter Nordlander for a critical reading of the manuscript and for helpful suggestions. This work was supported in part by The University of Tennessee, the U.S. Department of Energy (Grant No. DE-FG02-05ER46209), and by the LDRD Program of Oak Ridge National Laboratory, managed by UT-Battelle, LLC for the U.S. Department of Energy under DE-AC05-00OR22725. H. X. Xu also acknowledges financial support from the "100 Persons Project" of the Chinese Academy of Sciences.

[1] For recent review, see M. Moskovits, J. Raman Spectrosc. **36**, 485 (2005).
[2] H. X. Xu, E. J. Bjerneld, M. Käll, and L. Börjesson, Phys. Rev. Lett. **83**, 4357 (1999).
[3] A. M. Michaels, M. Nirmal, and L. E. Brus, J. Am. Chem. Soc. **121**, 9932 (1999).
[4] K. Kneipp, Y. Wang, H. Kneipp, L. T. Perelman, and I. Itzkan, Phys. Rev. Lett. **78**, 1667 (1997).
[5] S. Nie and S. R. Emory, Science **275**, 1102 (1997).
[6] R. D. Averitt, D. Sarkar, and N. J. Halas, Phys. Rev. Lett. **78**, 4217 (1997).
[7] W. Shi, Y. Sahoo, M. T. Swihart, and P. N. Prasad, Langmuir **21**, 1610 (2005).
[8] C. E. Talley, J. B. Jackson, C. Oubre, N. K. Grady, C. W. Hollars, S. M. Lane, T. R. Huser, P. Nordlander, and N. J. Halas, Nano Lett. **5**, 1569 (2005).
[9] E. Prodan, C. Radloff, N. J. Halas, and P. Nordlander, Science **302**, 419 (2003).
[10] R. A. Alvarez-Puebla, D. J. Ross, G.-A. Nazri, and R. F. Aroca, Langmuir **21**, 10504 (2005).
[11] H. X. Xu, Phys. Rev. B **72**, 073405 (2005).
[12] C. Sönnichsen, B. M. Reinhard, J. Liphardt, and A. P. Alivisatos, Nat. Biotechnol. **23**, 741 (2005).
[13] H. Metiu, Prog. Surf. Sci. **17**, 153 (1984).
[14] P. K. Aravind, A. Nitzan, and H. Metiu, Surf. Sci. **110**, 189 (1981).
[15] P. K. Aravind and H. Metiu, Surf. Sci. **124**, 506 (1983).

[16] H. X. Xu, J. Aizpurua, M. Käll, and P. Apell, Phys. Rev. E **62**, 4318 (2000).
[17] B. N. J. Persson, Chem. Phys. Lett. **82**, 561 (1981).
[18] A. Otto, Phys. Status Solidi A **188**, 1455 (2001).
[19] B. N. J. Persson, K. Zhao, and Z. Zhang, Phys. Rev. Lett. **96**, 207401 (2006).
[20] P. C. Waterman, Phys. Rev. D **3**, 825 (1971).
[21] D. W. Mackowski, J. Opt. Soc. Am. A **11**, 2851 (1994).
[22] J. Sinzig and M. Quinten, Appl. Phys. A **58**, 157 (1994).
[23] O. R. Cruzan, Q. Appl. Math. **20**, 33 (1962).
[24] S. Zou and G. C. Schatz, Chem. Phys. Lett. **62**, 403 (2005).
[25] P. B. Johnson and R. W. Christy, Phys. Rev. B **6**, 4370 (1972).
[26] C. L. Nehl, N. K. Grady, G. P. Goodrich, F. Tam, N. J. Halas, and J. H. Hafner, Nano Lett. **4**, 2355 (2004).
[27] H. X. Xu, Appl. Phys. Lett. **87**, 066101 (2005).
[28] L. L. Zhao, K. L. Kelly, and G. C. Schatz, J. Phys. Chem. B **107**, 7343 (2003).
[29] Q.-H. Wei, K.-H. Su, S. Durant, and X. Zhang, Nano Lett. **4**, 1067 (2004).
[30] U. Kreibig and M. Vollmer, *Optical Properties of Metal Clusters* (Springer, New York, 1995).
[31] K.-H. Su, Q.-H. Wei, X. Zhang, J. J. Mock, D. R. Smith, and S. Schultz, Nano Lett. **3**, 1087 (2003).
[32] Y. Lei and W.-K. Chim, J. Am. Chem. Soc. **127**, 1487 (2005).
[33] W. Wang and B. Gu, Appl. Spectrosc. **59**, 1509 (2005).
[34] M. A. De Jesús, K. S. Giesfeldt, J. M. Oran, N. A. Abu-Hatab, N. V. Lavrik, and M. J. Sepaniak, Appl. Spectrosc. **59**, 1501 (2005).